Supplementary Information

Title: **Low-Molecular-Mass Labile Metal Pools in *Escherichia Coli*: Advances using Chromatography and Mass Spectrometry**

Authors: Hayley N. Brawley and Paul A. Lindahl

Table of Contents:

Table S1. Standards for molecular mass calibration curve using single column.

Compound	Source	Method of detection	Molecular weight (Da)	Concentration	Log(MW)	Elution volume (mL)	V_e/V_o
$(Na)_2$AMP	see *Metal and ligand standards*	P, UV-260	347	100 µM	2.54	28.53	1.37
Riboflavin	Sigma Aldrich	UV-260	376	1 mM	2.58	26.59	2.65
NaADP	see *Metal and ligand standards*	P, UV-260	427	100 µM	2.63	25.87	1.55
$(Na)_2$ATP	see *Metal and ligand standards*	P, UV-260	507	100 µM	2.71	23.89	2.07
$(Na)_2$NADH	see *Metal and ligand standards*	P, UV-260	663	50 µM	2.82	24.67	2.44
$(Na)_4$NADPH	see *Metal and ligand standards*	P, UV-260	744	50 µM	2.87	22.74	2.57
Cyanocobalamin	Fisher Bioreagents	Co	1,355	50 µM	3.13	19.26	2.78
Insulin (bovine)	Sigma Aldrich	UV-280	5,734	50 µM	3.76	14.46	3.06
Cytochrome C (equine)	Sigma Aldrich	Fe	12,384	20µM	4.09	12.74	2.86
Thyroglobulin	Sigma Aldrich	UV-210	660,000	0.1 mg/ml	5.82	9.31	1.00
NaH_2PO_4	see *Metal and ligand standards*	Fe	95	20 µM	1.98	21.92	2.35
Cysteine	see *Metal and ligand standards*	S	121	500 µM	2.08	22.15	2.38
Methionine	see *Metal and ligand standards*	S	149	500 µM	2.17	21.19	2.28
GSH	see *Metal and ligand standards*	S	307	100 µM	2.49	21.09	2.27
ZnEDTA	Acros Organics/Sigma Aldrich	Zn	354	1/10 µM	2.55	19.74	2.12
Fe(Bipy)3	Fisher Chemical/Alfa Aesar	Fe, UV-523	524	2/20 µM	2.72	18.44	1.98
Fe(Phen)3	Fisher Chemical/Acros Organics	Fe, UV-510	597	2/20 µM	2.78	21.19	2.28
GSSG	see *Metal and ligand standards*	S	613	100 µM	2.79	20.03	2.15
Zn acetate (hexaaqua Zn)	see *Metal and ligand standards*	Zn	172	1 µM	2.24	44.89	4.82
$FeSO_4$ (hexaaqua Fe)	see *Metal and ligand standards*	Fe	164	1 µM	2.21	22.40	2.41
$MnCl_2$ (hexaaqua Mn)	see *Metal and ligand standards*	Mn	163	1 µM	2.21	20.71	2.22
$NiSO_4$ (hexaaqua Ni)	see *Metal and ligand standards*	Ni	166	1 µM	2.22	24.98	2.68

Zn (figure 1)		
Center (mL)	**Area (%)**	**FWHM (mL)**
(Ac) 20.3	26	1.4
(Ac) 21.9	15	1.0
(Ac) 24.1	30	3.3
(Ac) 26.1	4	1.4
(Ac) 31.3	25	4.5
(Ad) 20.2	2	1.8
(Ad) 23.9	1	3.3
(Ad) 25.7	0.4	2.0
(Ad) 30.5	2	4.5
Fe (figure 5)		
(Ab) 23.3	23	1.3
(Ac) 22.3	38	1.2
(Ac) 23.4	35	1.4
(Bb) 28.0	12	1.4
(Bc) 26.6	53	1.4
(Bc) 28.0	32	1.4
S (figure 6)		
Center (mL)	**Area (%)**	**FWHM (mL)**
20.1	28	1.6
21.1	51	1.2
21.3	14	0.8
22.1	7	1.4
P (figure 7)		
Center (mL)	**Area (%)**	**FWHM (mL)**
20.4	2	1.4
21.1	9	1.4
21.8	57	0.9
22.5	24	0.8
23.2	5	1.5
25.8	1	1.6
28.2	2	1.5
Fe (figure 9)		
Center (mL)	**Area (%)**	**FWHM (mL)**
(A) 20.4	51	2.0
(A) 21.8	18	1.2
(A) 23.6	24	3.3
(A) 26.1	2	1.4
(A) 28.3	5	4.6
(D) 20.4	6	1.6
(D) 21.9	3	1.1
(D) 23.6	4	2.8
(D) 25.9	1	1.4
Cu (figure 10)		
Center (mL)	**Area (%)**	**FWHM (mL)**
15.4	38	3.0
19.1	44	2.7
20.5	4	1.0
21.9	14	1.4
Mn (figure 11)		
Center (mL)	**Area (%)**	**FWHM (mL)**
20.2	32	0.9
21.2	68	0.9

Table S2. Parameters used to simulate chromatography peaks. FWHM, full width at half maximum. The areas listed for simulations of Figures 1Ad and 9D do not sum to 100% because the dominant peaks in those traces were no

Figure S1. Zinc-detected chromatographic traces of individual batches of FTS. Replicates are listed in order from highest OD_{600} (top) at which cells were harvested to lowest (bottom). Blue horizontal lines separate the different exponential growth phases. Dashed vertical lines highlight LMM Zn species with V_e/V_o. R1-R10 are individual batches numbered chronologically.

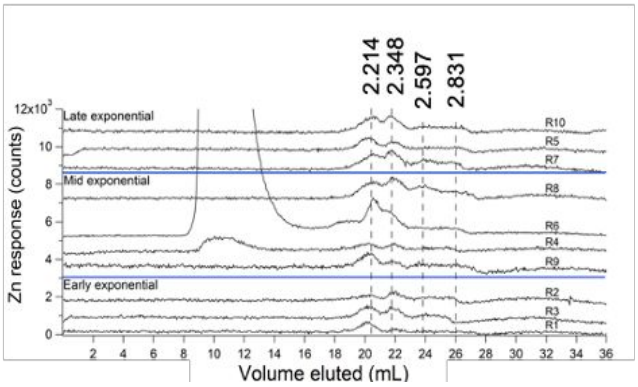

Figure S2: Phosphorus-detected chromatographic traces of Na_2ATP using 50 mM AA (A) or 20 mM AA (B) as the mobile phase. In A and B, the solid-line traces were from solutions containing 1 μM $FeSO_4$ + variable (final) concentrations of Na_2ATP, as follows in units of μM ATP. Panel A and B: (a), 5 ×200; (b), 10 ×100; (c), 25 ×40; (d), 50 ×20; (f), 500 ×2; (g), 1000. In A and B, the dashed-line traces were from solutions of Na_2ATP without added iron at the following concentrations (μM): Panel A and B: (a), 5 ×200; (b), 10 ×100; (c), 25 ×40; (d), 50 ×20; (e), 100 ×10; (f), 500 ×2; (g), 1000.

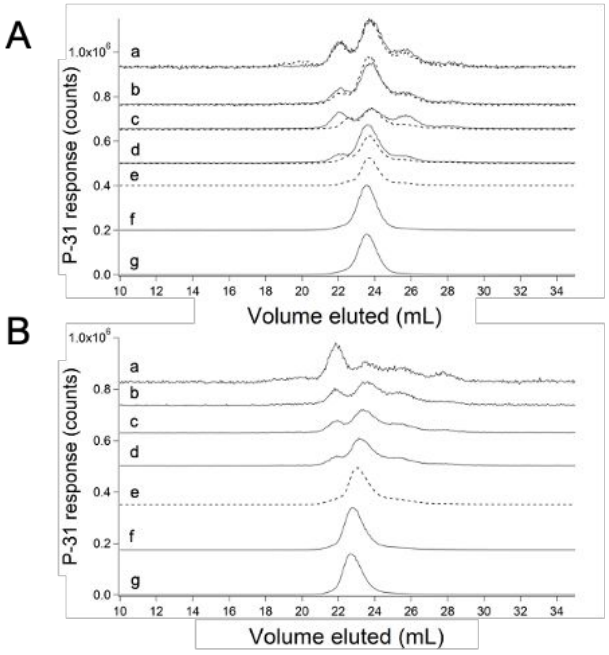

Figure S3. Zinc- and Sulfur-detected traces showing no Zn(GSH) complex in cytosolic FTS. (A), averaged FTS from cells supplemented with 100 µM Zn acetate (green line, Zn detected; blue line, S detected); (B), 100 µM GSH (blue) ×3 and 2 µM Zn acetate (green); (C), 2 µM Zn acetate (green) + 1 mM GSH (blue); (D), 2 µM Zn acetate (green) + 100 mM GSH (blue ÷100). Traces (B) – (D) were standards prepared in mobile phase buffer.

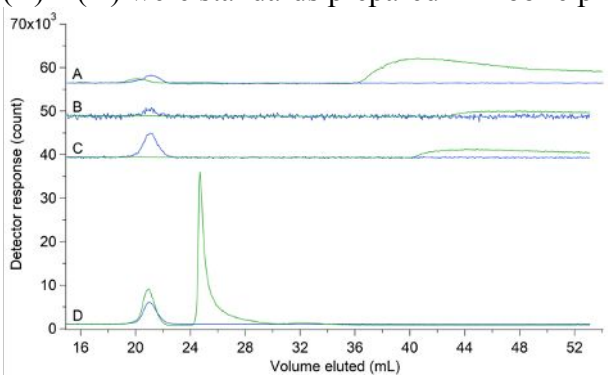

Figure S4. Sulfur-detected chromatographic traces of individual batches of FTS. Replicates in order from highest OD_{600} (top) at which cells were harvested to lowest (bottom). Blue horizontal lines separate the different exponential growth phases. Dashed vertical lines highlight LMM S species with V_e/V_o.

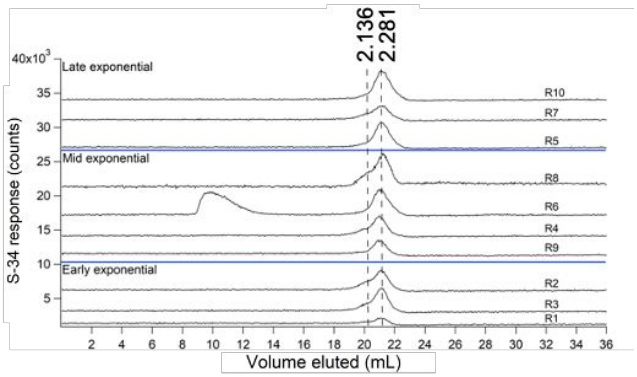

Figure S5. Positive mode ESI-MS spectra showing Sulfur-containing metabolites in cytosolic FTS. (A), Sulfur-detected averaged FTS from cells collected on the double peptide column (dashed lines indicated fraction boundaries). (B), Positive mode ESI of selected fractions from (A). Peaks within each column have been normalized to the largest peak intensity.

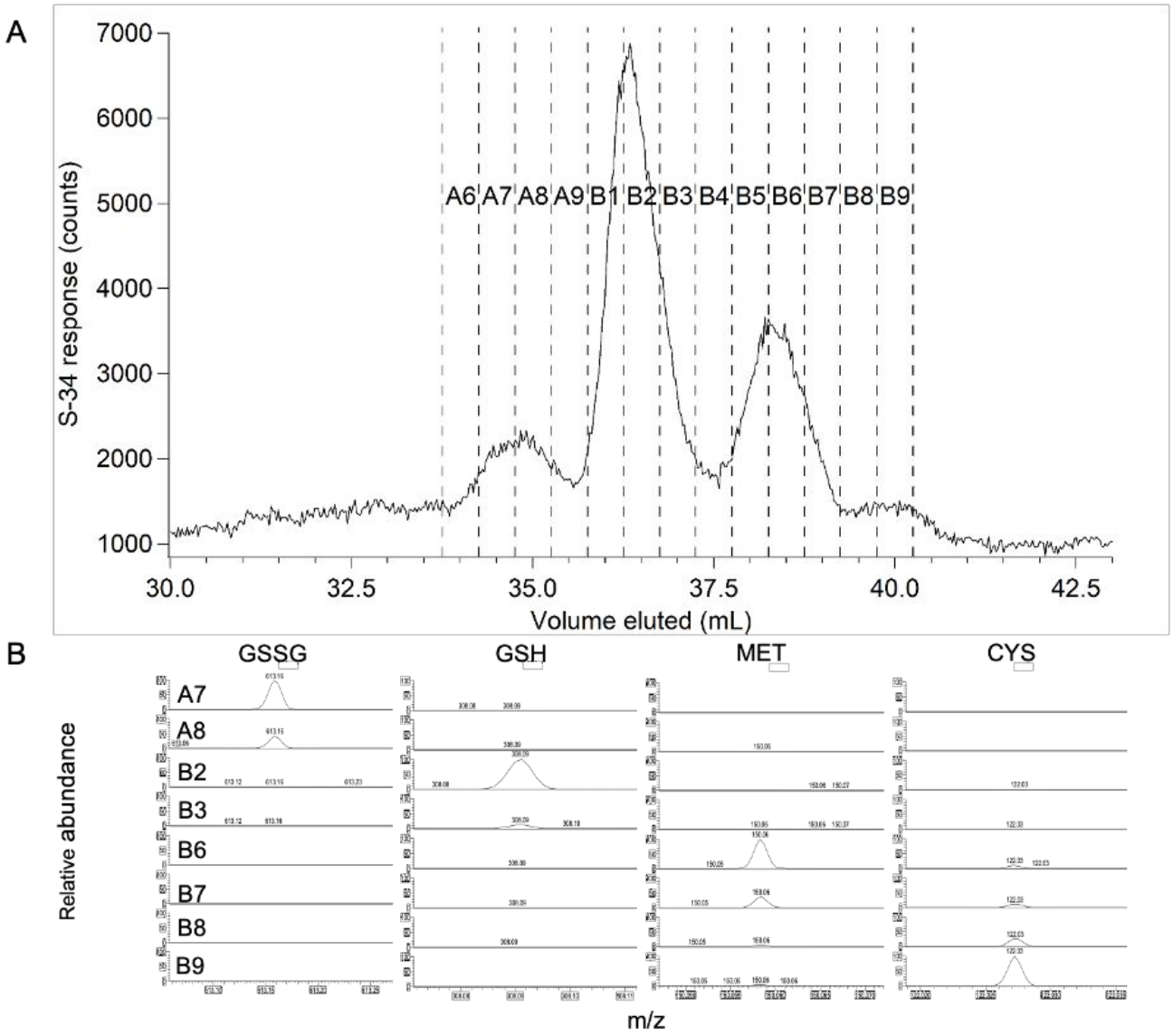

Figure S6. Phosphorus-detected chromatographic traces of individual batches of FTS. Panel A: replicates in order from highest OD_{600} (top) at which cells were harvested to lowest (bottom). Panel B: Same replicates as in Panel A with main peak removed. Blue horizontal lines separate the different exponential growth phases. Dashed vertical lines highlight LMM P species with V_e/V_o.

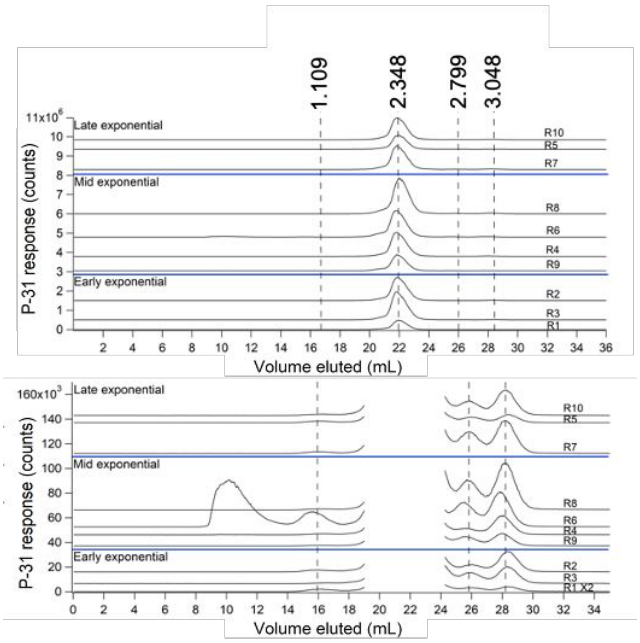

Figure S7. Negative mode ESI-MS spectra showing Phosphorus-containing metabolites in cytosolic FTS. (A), Phosphorus-detected averaged FTS from cells collected on single peptide (dashed lines indicated fraction boundaries). The offset line is the ICP-MS data magnified ×20 excluding the dominating peak. (B), Negative mode ESI of selected fractions from (A). Peaks within each column have been normalized to the largest peak intensity.

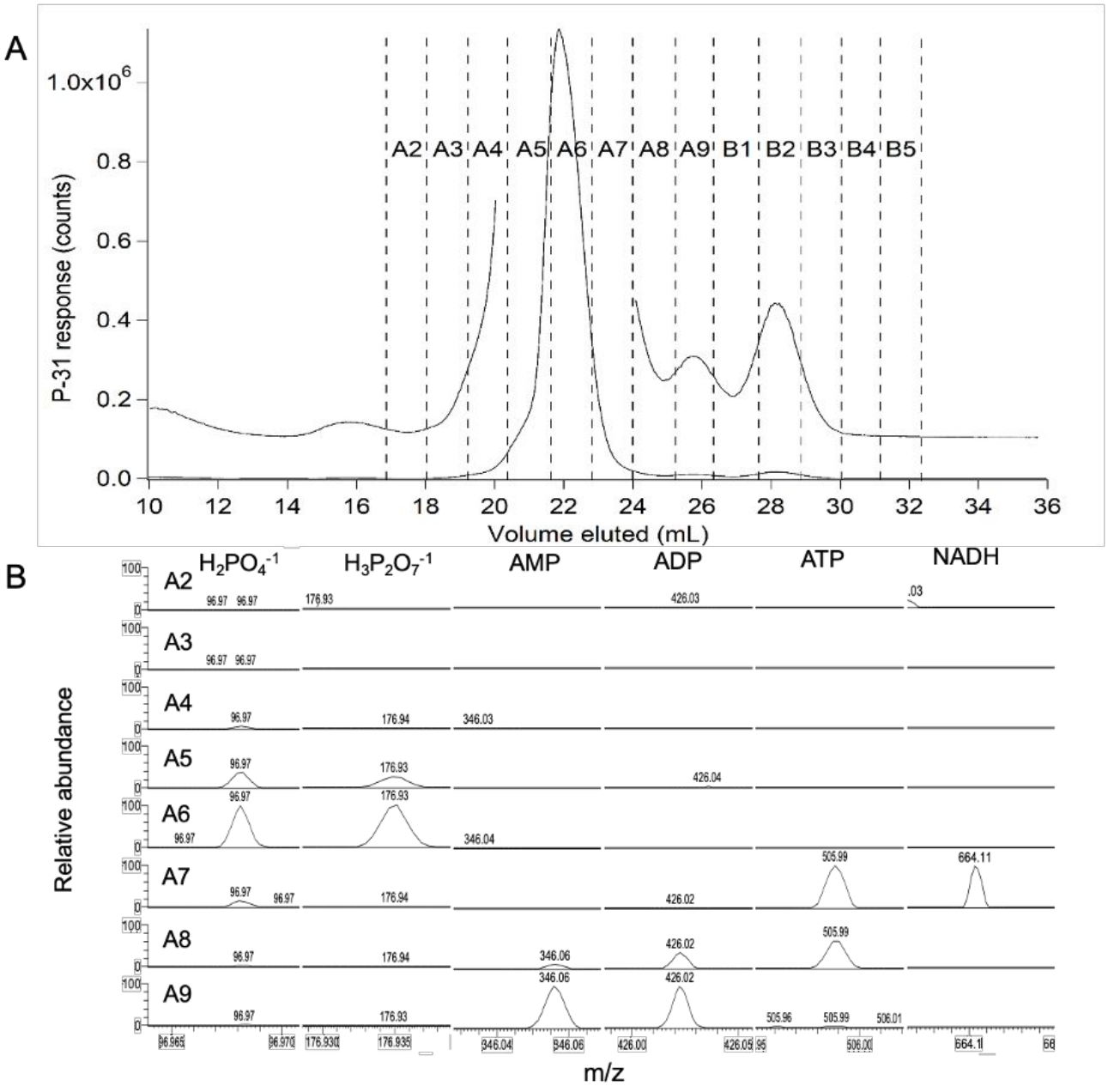

Figure S8. Positive mode ESI-MS spectra showing salt suppression of GSH. (A), 500 µM GSH; (B), a FTS replicate 8 (R8) (C), the sulfur-containing fraction collected from the FTS replicate in (B); (D), 500 µM GSH + 25 mM Na_2HPO_4; (E), 500 µM GSH + 25 mM KH_2PO_4; (F), 500 µM GSH + 25 mM NaCl; (G), 500 µM GSH + 25 mM $MgSO_4$. Spectra were normalized to the peak intensity of the GSH standard in (A). Relative percentage intensities for (B) – (G) are indicated.

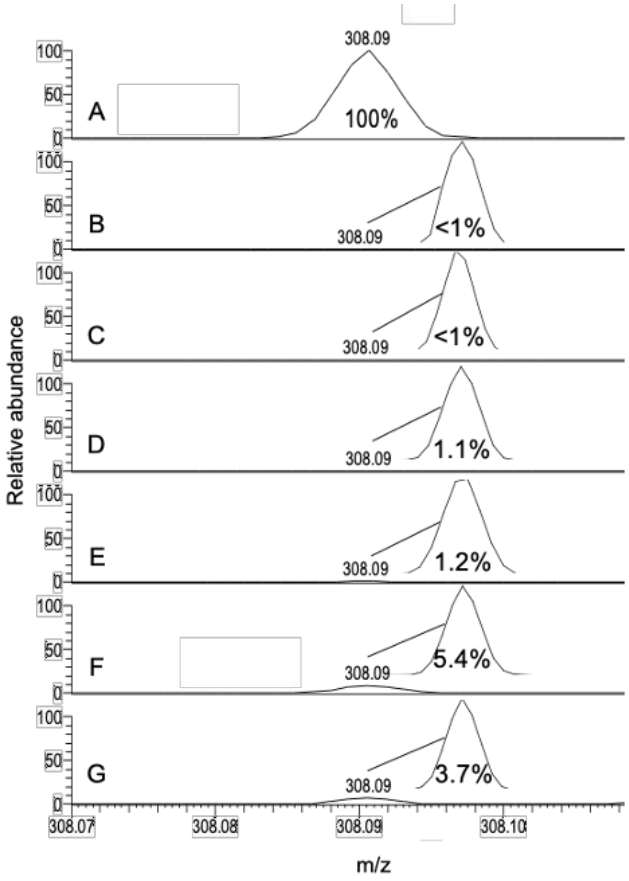

Figure S9. Iron-detected chromatographic traces of individual batches of FTS. Replicates in order from highest OD_{600} (top) at which cells were harvested to lowest (bottom). Blue horizontal lines separate the different exponential growth phases. Dashed vertical lines highlight LMM Fe species with V_e/V_o.

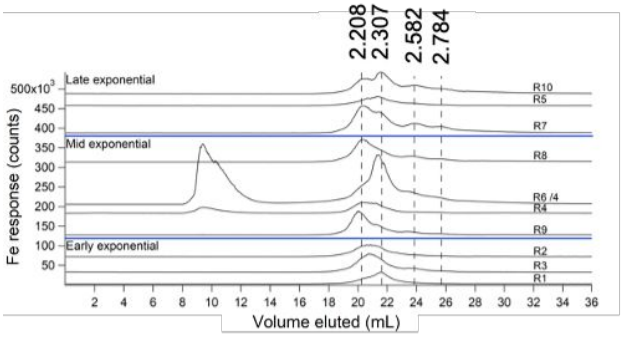

Figure S10. Acid phosphatase chelates metals from LMM metal complexes. Solid, dark-colored traces are the average of 8-10 FTSs for Fe (red, ÷4), Zn (green), Cu (blue), Mn (pink), and P (black, ÷100). Solid, light-colored traces are FTS + 2 mg/mL acid phosphatase for (same scaling for average FTSs). Dashed traces are metal content of standard 2 mg/mL acid phosphatase.

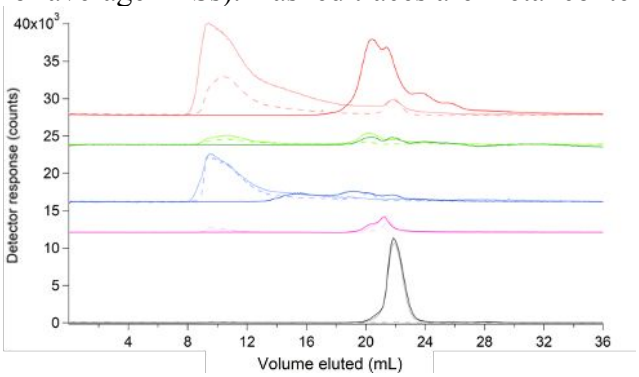

Figure S11. Copper-detected chromatographic traces of individual batches of FTS (R1 – R10). Replicates in order from highest OD_{600} (top) at which cells were harvested to lowest (bottom). Blue horizontal lines separate the different exponential growth phases. Dashed vertical lines highlight LMM Cu species with V_e/V_o.

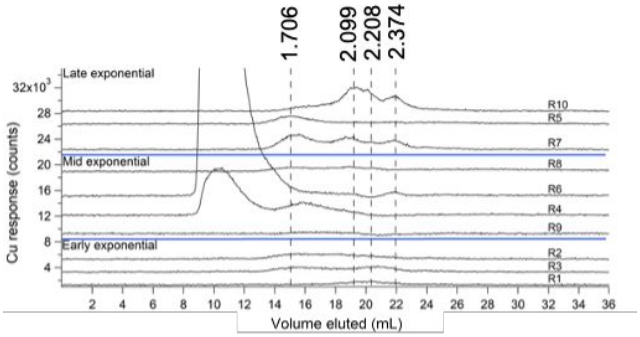

Figure S12. Manganese-detected chromatographic traces of individual batches of FTS (R1 – R10). Replicates in order from highest OD_{600} (top) at which cells were harvested to lowest (bottom). Blue horizontal lines separate the different exponential growth phases. Dashed vertical lines highlight LMM Mn species with V_e/V_o.

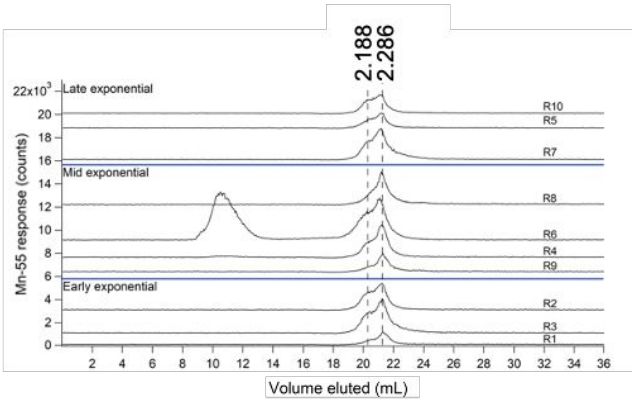

Figure S13. Average of 9 – 10 FTS traces of Ni (purple), S (yellow), and P (black) ÷100. The offset line in the bottom trace has been magnified ×10 with the dominating peak excluded.